Published in final edited form as:
Biochemistry. 2006 June 27; 45(25): 7854–7860. doi:10.1021/bi0601510.

A Conserved Quadruplex Motif Located in a Transcription Activation Site of the Human c-kit Oncogene

Himesh Fernando[‡], **Anthony P. Reszka**[§], **Julian Huppert**[‡], **Sylvain Ladame**[‡], **Sarah Rankin**[§], **Ashok R. Venkitaraman**[‖], **Stephen Neidle**[§], and **Shankar Balasubramanian**[*,‡]

[‡] Department of Chemistry, University of Cambridge, Lensfield Road, Cambridge, CB2 1EW, United Kingdom.

[§] Cancer Research UK Biomolecular Structure Group, The School of Pharmacy, University of London, 29-39 Brunswick Square, London WC1N 1AX, United Kingdom.

[‖] MRC Cancer Cell Unit, Hutchison/MRC Research Centre, University of Cambridge, Hills Road, Cambridge CB2 2XZ, United Kingdom

Abstract

The c-kit gene encodes a receptor tyrosine kinase, whose engagement by its ligand triggers signals leading to cell proliferation. c-kit activity is elevated in gastrointestinal stromal tumors (GISTs), and its therapeutic inhibition by small molecules such as imatinib is clinically validated. We identified a putative quadruplex forming 21-nucleotide sequence upstream of the c-kit transcription initiation site (c-kit21), on the G-rich strand, which occupies a site required for core promoter activity. Here, we show by nuclear magnetic resonance (NMR), circular dichroism (CD), and ultraviolet (UV) spectroscopic methods that c-kit21 forms quadruplexes under physiological conditions. Mutational analysis of c-kit21 has provided insights into its structural polymorphism. In particular, one mutated form appears to form a single quadruplex species that adopts a parallel conformation. The quadruplex-forming sequence shows a high level of sequence conservation across human, mouse, rat, and chimpanzee. The small variation in sequence between the quadruplex in human/chimpanzee as compared to the rat/mouse was examined more closely by biophysical methods. Despite a variation in the sequence and length of loop 2, the quadruplexes showed both comparable CD spectra, indicative of parallel quadruplexes, and also similar thermal-stability profiles, suggesting conservation of biophysical characteristics. Collectively, the evidence suggests that this quadruplex is a serious target for a detailed functional investigation at the cell-biology level.

It was first proposed over 4 decades ago that guanine bases can associate in a cyclic arrangement to form planar arrangements of four guanines, G-quartets (1), in which each guanine is bonded to two neighboring guanines via hydrogen bonds (2). These G-quartets enable DNA sequences rich in guanines to form complex-folded structures, “quadruplexes”, that are further stabilized by cations. The biological relevance of quadruplexes is now being intensively investigated, largely as a consequence of the identification of quadruplex-forming sequences in the genome. Tandem-repeat sequences in the telomeres of humans (3), *Oxytricha* (4), and *Tetrahymena* (5) have been shown to form quadruplex structures. These have also been proposed in immunoglobin switch regions (6), within human

---

[*]To whom correspondence should be addressed. E-mail: sb10031@cam.ac.uk..

SUPPORTING INFORMATION AVAILABLE A table showing half-transition temperatures at different strand concentrations and a figure showing half-transition temperatures of c-kit21 and mouse/rat c-kit sequences at different K^+ concentrations. This material is available free of charge via the Internet at http://pubs.acs.org.

Europe PMC Funders Author Manuscripts

immunodeficiency virus (HIV) RNA (7), as well as in a variety of RNA and DNA aptamers (8). Quadruplexes in the promoter region of genes have been proposed for Ki-ras (9), c-myc (10, 11), VEGF (12), and HIF-1α (13).

Biophysical evidence exists in support of quadruplex formation for a small number of sequences in vitro. The evidence for quadruplex existence in cells is indirect and more limited but increasing. There is evidence of the existence of several telomeric quadruplex-binding proteins, which include RAP 1 (14, 15) and the β subunit of *Oxytricha* telomere-binding protein (16). Recently, it was demonstrated that telomere end-binding proteins in the ciliate *Stylonychia* can bind and regulate the formation of G-quadruplex structures in cells. Furthermore, quadruplex formation was under the control of a cell-cycle-dependent phosphorylation event (17). Quadruplex-binding proteins are also found in diverse organisms including humans, yeast, *Escherichia coli*, and the *Arabidopsis* plant (18). The discovery of quadruplex-binding proteins in *E. coli*, which lacks telomeres and has a circular chromosome, implies that quadruplex structures may exist in the double-stranded circular chromosomes (18). Studies using electron microscopy suggest that plasmids containing mammalian sequences form G-quadruplex structures during transcription of the C-rich strand (19).

Quadruplexes can be broadly categorized as either interor intramolecular and further classified according to the orientation of the strands, which may be parallel or antiparallel. Nuclear magnetic resonance (NMR) spectroscopy and X-ray crystallography are robust methods for elucidating quadruplex topology but to date have only succeeded in elucidating a small number of quadruplex structures. Biophysical techniques such as circular dichroism (CD) spectroscopy (20) and ultraviolet (UV) thermal difference spectra (21-23) can also provide valuable insights into quadruplex conformation.

A putative promoter quadruplex reported for the c-myc oncogene (10) has recently received considerable attention. The 27 base-pair nuclease hypersensitive element III_1 (NHE III_1) of the c-myc promoter controls 80–90% of c-myc transcription (10). It has been suggested that the NHE III_1 element equilibrates between transcriptionally active and silenced forms and that the silenced form corresponds to a quadruplex (24, 25). Expression of c-myc can be suppressed with quadruplex-stabilizing molecules (11). This is a proof of concept that expression of genes can be downregulated by the formation of quadruplexes in the promoter region of the gene, at least in a model system. The proposed quadruplexes in VEGF and HIF-1α gene promoters overlap with binding sites for transcription factors (12, 13). This raises the possibility of ligand-mediated stabilization of quadruplexes to prevent the binding of transcription factors and potential regulation of gene expression.

We report here a putative promoter quadruplex for the c-kit oncogene, which codes for a tyrosine kinase receptor (26). c-kit function is pivotal for relaying an extracellular signal in response to the binding of its ligand, stem cell factor (SCF). When activated, kit stimulates proliferation, differentiation, migration, and survival (27). Kit is similar in structure to other receptor tyrosine kinases and highly expressed in haematopoietic stem cells, mast cells, melanocytic cells, germ cells, and interstitial cells of Cajal (28). Specific mutations in the c-kit gene lead to ligand-independent activation or constitutive activation of the c-kit protein, which results in uncontrolled cell proliferation. This is considered the primary pathogenic event in gastrointestinal stromal tumors (28).

The human c-kit promoter lacks both a TATA box (29) and a CCAAT box (30). It contains several potential Sp1-binding sites (26), of which a sequence stretch situated from −121 to −130 bp upstream of the transcription initiation site (Figure 1A) is essential for core promoter activity (31). Promoter deletion assays have shown that the sequence from −120 to

−161 bp upstream of the transcription initiation site is crucial for maximal core promoter activity in a nontissue-specific manner (31). Transcriptional regulation of c-kit expression is complex, involving several activators and repressors (32).

On the basis of the literature and biophysical studies of quadruplex-forming sequences carried out in our laboratory, algorithms have been developed that can screen sequences within genomes that may form quadruplexes (33, 34). Two such sequences have been identified by us within the c-kit promoter region, one positioned between −87 and −109 bp and the other positioned between −140 and −160 bp upstream of the transcription initiation site. The former has been shown by us to fold into a quadruplex in vitro (35).

We have now analyzed in detail this second putative quadruplex-forming sequence, d(CGGGCGGGCGCGAGGGAGGGG) (c-kit21). There are two features of c-kit21 that lead us to believe it is likely to have biological function. First, it occupies a region within a 42-base fragment essential for core promoter activity (31) (Figure 1A). Second, this putative quadruplex sequence is highly conserved in human, mouse, rat, and chimpanzee (Figure 1B). The four tracts of 3G each are unchanged, with the main variations being present in the sequence of loop 2. Furthermore, the location of the putative quadruplex, relative to the transcription initiation site, is identical in human and chimpanzee (137 bases upstream) and close (98 bases upstream) in mouse and rat.

Until now, kinase-targeted cancer therapies such as Gleevec (an inhibitor that has activity against the c-kit kinase as well as the abl kinase) (36) all inhibit the kinase protein after it has been expressed rather than control its expression. The positioning of this putative quadruplex makes it a potentially attractive target to be exploited for the regulation of c-kit at the transcriptional level. We report here studies with a range of biophysical techniques to probe the structure and stability of this conserved putative c-kit quadruplex element.

MATERIALS AND METHODS

Sample Preparation

The DNA oligonucleotide samples d($CG_3CG_3CGCGAG_3AG_4$) (c-kit21), d($CG_3CG_3CGCGAG_3ATG_3$) (c-kit18T), and d($CG_3CG_3CGCGAG_3AG_3T$) (c-kit21T) were synthesized on an applied Biosystems DNA synthesizer using solid-phase β-cyanoethylphosphoramidite chemistry. The oligonucleotides were deprotected and cleaved from the solid support by immersing the resin in concentrated degassed ammonia solution at 60 °C overnight. The crude oligonucleotides were purified using HPLC on a BioCAD workstation with an Oligo R3 column (PerSeptive Biosystems, Inc.). The oligonucleotides were then lyophilised and dialyzed against double-distilled water and lyophilised again to produce a final purified oligonucleotide. Absorbance of 1:100 diluted samples in distilled water was measured at 260 nm to determine the concentration.

NMR Spectroscopy

NMR experiments were performed on a 500 MHz Bruker Avance spectrometer with a 5 mm Triple Resonance Inverse (TCI) cryoprobe. Water suppression was achieved using the Watergate W5 pulse sequence. Samples were prepared to a final oligonucleotide concentration of 1 mM in 20 mM potassium phosphate buffer (pH 7.0) and 10% D_2O containing varying KCl concentrations up to 100 mM. The samples were heated to 90 °C for 10 min, annealed over a period of 14 h at a rate of 0.1 °C/min down to 4 °C, and maintained at 4 °C overnight. Spectra were recorded at 27, 35, and 43 °C. Temperatures above 43 °C could not be reached because of limitations in the cryoprobe.

UV Spectroscopy

All UV experiments were performed on a Cary Varian UV/vis spectrophotometer. The thermal melting curves were obtained at 295 nm. Samples were prepared to final oligonucleotide concentrations of 1–40 μM in 10 mM Tris-HCl (pH 7.0) containing 100 mM KCl. The DNA samples were annealed by heating at 90 °C for 10 min and slow cooling to 4 °C at a controlled rate of 0.1 °C/min. Samples were degassed for 1 min, and 400 μL was transferred to a clear cuvette of 1 cm path length. Data were recorded every 0.5 °C during heating and cooling, which were carried out at a rate of 0.25 °C/min. Dependent upon whether the UV thermal melting curves are superimposable (reversible folding and unfolding) or not (nonreversible folding and unfolding), the equilibrium T_m or half-transition temperature ($T_{1/2}$) were determined respectively using van't Hoff (21) and first derivative methods.

UV thermal difference spectra were obtained by carrying out a wavelength scan from 340 to 220 nm above (85 °C) and below (20 °C) the thermal transition temperature and plotting the difference in absorbance at each wavelength. The data were then normalized relative to the highest positive peak.

CD Spectroscopy

CD spectra were obtained on a Jasco J-810 spectropolarimeter. The wavelength was varied from 220 to 320 nm at a rate of 50 nm/min. Measurements were made at 20 °C using a quartz cell, with a path length of 1 cm. Each spectrum reported is an average of five scans. The samples were prepared to a final oligonucleotide concentration of 4 μM in 10 mM Tris-HCl (pH 7.0) and 100 mM KCl. Annealing was done the same as for UV samples. For each experiment, a CD spectrum of the buffer was recorded and subtracted from the spectrum obtained for the DNA-containing solution.

RESULTS

NMR Study on the Native c-kit21 Sequence

NMR spectroscopy has been used extensively to confirm the presence of the quadruplex structure in nucleic acids (37). In particular, the imino protons of guanines involved in G-tetrad formation have characteristic resonances that appear between 10.5 and 12 ppm in a ^{1}H NMR spectrum, owing to the formation of specific hydrogen bonds to O6 of adjacent guanines. The one-dimensional (1D) ^{1}H NMR spectrum of c-kit21 in 90% H_2O and 10% D_2O (Figure 2A) displays a broad envelope with some fine structure between 10.5 and 12 ppm. While a single quadruplex intramolecular conformation can display sharp imino resonance (38), the spectrum shown in Figure 2A is more suggestive of multiple interconverting quadruplex conformations (39), where the interconversion rate is comparable to the NMR time scale.

UV Thermal Difference Spectrum and Melting Analysis

Intramolecular G-quadruplex structures exhibit characteristic patterns in the UV differential spectra, which can indicate the presence of quadruplexes (21-23). The difference spectrum obtained for c-kit21 exhibits two positive maxima at 240 and 277 nm, a shoulder at 255 nm, and a negative minimum at 296 nm (Figure 3), which is comparable to thermal difference spectra obtained for other known quadruplexes (22, 23).

The stability of G-quadruplexes can be determined by conducting UV thermal melts at 295 nm, where melting is accompanied by a hypochromic shift (21). The T_m or $T_{1/2}$ values relate to the stability of the folded quadruplex, and the nature of the melting and cooling spectra can provide insights into the folding/unfolding kinetics and intra/intermolecular nature of the

quadruplex (21). The melting and cooling curves for c-kit21, in K^+ buffer (Figure 4), show a single transition with a $T_{1/2}$ of 70 ± 1 °C. This $T_{1/2}$ is higher than that of the human telomeric sequence (H-telo) of 58 °C in Na^+ and 63 °C in K^+ (40) under comparable conditions but is lower than that for the c-myc quadruplex (T_m > 80 °C) (38).

UV thermal melting analysis was conducted with a wide range of oligonucleotide concentrations from 1 to 40 μM (see the Supporting Information). The results indicate that the $T_{1/2}$ of the c-kit21 quadruplex is independent of the strand concentration, which is consistent with an intramolecular quadruplex.

The effect of the K^+ concentration on the $T_{1/2}$ was also investigated. It is apparent from the data (see the Supporting Information) that the quadruplex becomes more stable with increasing K^+ concentration, with stability saturating at K^+ concentrations above 100 mM. This K^+ dependence is consistent with the pattern of stabilization observed for other quadruplexes that include the human telomeric (21) and c-myc (38) quadruplexes. The dependence of cation type on stability is indicated in Table 1, where the $T_{1/2}$ values suggest stabilization in the order $K^+ > Na^+ > Li^+$, which is typical of cation preference for quadruplexes (21).

CD Study of c-kit21

CD spectroscopy can provide insights into the strand orientation of quadruplexes, where parallel and antiparallel orientations are known to result in characteristically distinct spectra (20). Parallel-stranded quadruplexes typically have a positive signal at 260 nm and a negative signal at 240 nm, whereas the antiparallel quadruplexes exhibit a positive signal at 295 nm and a negative signal around 260 nm. Sequences capable of forming both conformations, or indeed a mixed conformation, can produce a hybrid of parallel and antiparallel spectra often with maxima at both 260 and 295 nm. The spectrum produced by the c-kit21 sequence (Figure 5) appears to have a strong signal peak at 263 nm with a weak peak at 295 nm. This indicates a predominant parallel conformation with the possibility of a small proportion of antiparallel structure(s).

Reducing Heterogeneity by Mutations

The native c-kit21 sequence has four G-tracts, of which the first three each contain three guanines, whereas the fourth G-tract contains four guanines, suggesting some potential ambiguity as to which guanines in the fourth tract participate in tetrad formation. We reasoned that systematic replacement of a guanine from either end of the fourth G-tract may reduce the heterogeneity of quadruplexes formed. Therefore, guanine to thymine mutations were made at positions 18 (c-kit18T) and 21 (c-kit21T) of the c-kit21 sequence (Figure 1C).

c-kit18T Is Less Heterogeneous than c-kit21

The G18T mutation not only restricts the number of guanines but also fixes the length of the third loop to two nucleotides. This had a consequence on the NMR and CD spectra and also the T_m value. The 1D ^{1}H NMR spectrum of the c-kit18T derivative (Figure 2B) shows improved resolution and is devoid of the broad envelope in the imino proton region compared to the native sequence spectrum, suggesting the presence of fewer conformers in equilibrium. UV thermal melting of c-kit18T shows a drop in T_m by 10 °C (Figure 4) relative to that of c-kit21. The CD spectrum of c-kit18T (Figure 5A) suggests that it forms a largely parallel conformation but indicates the presence of some antiparallel character as well.

c-kit21T Forms a Homogeneous Quadruplex

The G21T mutation was designed to unambiguously restrain the length of the third loop to a single nucleotide and the fourth G-tract to three guanines. This modification had a significant effect on the biophysical properties of the folded quadruplex. The NMR spectrum of c-kit21T shows fine structure (Figure 2C) with the sharpest peaks having line widths of around 5 Hz, suggestive of the homogeneous quadruplex structure. This is confirmed by the presence of 11 imino resonance peaks in the 10.5–12 ppm region, of which the large peak at 11.14 ppm integrates to two protons. The number and intensity of the resonances signify the 12 guanines of the 3 tetrads, indicating a single quadruplex. The CD spectrum exhibited by c-kit21T (Figure 5A) suggests a parallel quadruplex with negligible signal intensity at 295 nm. UV melting analysis of c-kit21T shows a reversible melting transition with a T_m value of 68 ± 1 °C (Figure 4).

Thermal Difference Spectra of Modified Sequences

The thermal difference spectra of c-kit18T and c-kit21T were similar to that of c-kit21 and had their maximum and minimum peaks centered at the same wavelength values (240, 275, and 295 nm) (Figure 3A). In addition, the close resemblance of c-kit21 and c-kit21T spectra could indicate similarities in quadruplexes formed by their sequences. The CD spectra (Figure 5A) and $T_m/T_{1/2}$ values of c-kit21 (70 ± 1 °C) and c-kit21T (68 ± 1 °C) also support this argument, with the c-kit21T CD spectrum almost superimposing the spectrum produced by c-kit21 and $T_m/T_{1/2}$ values being close to one another.

CD and UV Properties of the Mouse/Rat c-kit Quadruplex

The corresponding putative quadruplex sequence in mouse/rat does show some differences in loop 2, which is only four nucleotides long, rather than five, and also a quite different sequence comprised entirely of purines. We have recently found that loop length (41) and also loop sequence (35) can have a profound influence on quadruplex formation. Therefore, we analyzed the mouse/rat c-kit quadruplex using UV melting analysis and CD spectroscopy. These biophysical experiments suggest that the mouse/rat c-kit motif also folds into a quadruplex (Figures 3B and 5B). The UV thermal melting analysis carried out at different K^+ concentrations gives a stability profile that is indistinguishable from that of the human native c-kit sequence (c-kit21) (see the Supporting Information). At 100 mM K^+ concentration, the $T_{1/2}$ values for human c-kit21 and mouse/rat quadruplex sequences were 70 ± 1 and 69.5 ± 1 °C, respectively. The thermal difference spectrum (Figure 3) exhibits positive and negative peaks centered around typical values for quadruplexes (22, 23). The CD spectrum demonstrates a signature similar to that shown by the human c-kit21, which consists of strong parallel and weak antiparallel signals (Figure 5).

DISCUSSION

The combined data obtained from NMR, CD, and UV spectroscopic analyses show that the genomic DNA sequence c-kit21 folds into quadruplex structures under near physiological conditions. The UV melting analysis of c-kit21 showed the expected K^+ ion concentration dependence and cation preference $K^+ > Na^+ > Li^+$. Furthermore, the $T_{1/2}$ value of 70 ± 1 °C in 100 mM K^+ suggests that the intramolecular quadruplex formed by c-kit21 is relatively stable compared to the human telomeric quadruplex (63 °C in K^+) (40), under comparable conditions, but not as stable as the c-myc quadruplex (T_m > 80 °C) (38).

To address the apparent structural heterogeneity of quadruplexes formed by c-kit21, we studied two mutated forms. The mutated sequence c-kit21T forms a single structure, as judged by 1D ^1H NMR, and CD spectroscopy suggests a parallel-folded topology. The other mutated sequence, c-kit18T, gave an NMR spectrum consistent with fewer structures than c-

kit21, with the associated CD spectrum of c-kit18T suggesting the presence of mainly parallel quadruplex with some antiparallel quadruplex. In a related study on the NHE III_1 of c-myc, a mutated quadruplex (myc-1245) was generated with loops 1 and 3 consisting of a single nucleotide and loop 2 with six nucleotides, where the mutated quadruplex was shown to fold into a single propeller-type quadruplex (38). The similarities in loop lengths and the CD data suggest that the c-kit21T structure should be analogous. The fact that the mutant c-kit18T, with three guanines in the fourth stretch akin to c-kit21T, did not show a single dominant structure, demonstrates that simply distributing the 12 guanines into four tracts of 3 guanines each is not sufficient to form a single quadruplex species. Rather, this study suggests that loop length was the significant factor to influence quadruplex heterogeneity. Studies on the loop-length dependence of quadruplexes by Hazel et al. further corroborate this argument (41). c-kit21T has loop lengths of 1, 5, and 1 nucleotides, whereas c-kit18T has loop lengths 1, 5, and 2 nucleotides. Therefore, the only difference in the c-kit18T from the c-kit21T is an additional nucleotide in the third loop. We have previously shown (41) that the presence of one loop with a single residue favors a topology with at least one double-reversal loop being formed. In principle, a dinucleotide loop can be involved in both fold-back and double-reversal loops (38, 39, 41). On this basis, one would expect the presence of two single-nucleotide loops to push the equilibrium of possible quadruplex conformations toward a parallel topology as a result of steric hindrance to antiparallel-type structures and short diagonal loops. We believe that the increased size of the third loop present in c-kit18T may be responsible for the mixture of parallel and antiparallel quadruplex character suggested by the CD spectrum. The UV data also suggests that a two-nucleotide third loop in c-kit18T significantly destabilizes the quadruplex relative to a single-nucleotide loop in c-kit21T.

The heterogeneous population of quadruplexes observed for the native sequence c-kit21 is likely to include the subpopulations observed for c-kit18T and c-kit21T and thus contain both parallel and antiparallel quadruplexes. On the basis of CD spectra, UV thermal difference spectra, and the UV thermal melting transitions, it can be seen that the properties of native sequence c-kit21 most closely resemble those of c-kit21T, rather than c-kit18T, which may suggest that the c-kit21 population is dominated by the quadruplex conformation formed by c-kit21T.

A noteworthy feature of the human c-kit21 motif is that it is absolutely conserved in chimpanzee and a closely related sequence is also found in mouse/rat at a similar location with respect to the transcription start site. Sequence conservation can be taken as an indication of functional relevance of a sequence stretch. However, because our working hypothesis is quadruplex-based, we explored and compared the quadruplex-related properties of the mouse/rat c-kit motif. The mouse/rat c-kit motif forms a quadruplex, as judged by UV and CD analyses. CD spectroscopy suggests the mouse/rat motif has a parallel-folded configuration, analogous to the human motif. Furthermore, the mouse/rat c-kit quadruplex has thermal stability properties that are identical to those of the human c-kit sequence. The apparent conservation of these measurable quadruplex-related properties, despite some apparent divergence in loop 2, is suggestive of quadruplex-related function.

CONCLUSION

The G-rich strand of the promoter region of c-kit forms a mixture of stable quadruplexes under near physiological conditions. The proximity of the sequence to the likely binding site of the transcription factor Sp1 (31) and its requirement for core promoter activity suggest that it may be worthy of consideration as a potential drug target for the regulation of c-kit transcription. The fact that the c-kit21 quadruplex sequence is conserved in several species and that they all fold into quadruplexes in vitro with similar biophysical properties could be

suggestive of its biological function. We also note that our previous findings, which suggest quadruplex-forming sequences are likely to have at least one single-nucleotide loop (33), are upheld for c-kit21 and also hold for the previously studied genomic quadruplexes from c-kit (35), c-myc (10, 11), VEGF (12), and HIF-1 (13). High-resolution structural data is only available to date on the c-myc quadruplex (38, 39), showing that it conforms to the parallel quadruplex motif, although parallel folds have also been suggested for the VEGF and HIF-1 quadruplexes on the basis of CD and chemical-footprinting data. This is not unexpected in view of our findings (41) that parallel topology is the consequence of single-nucleotide loops. Cell-biological studies to explore the functional relevance of the c-kit quadruplex described in this paper are now underway and will be reported in the future.

Acknowledgments

We thank Drs. Yamuna Krishnan-Ghosh, John Christodoulou, and Pravin Shirude for assistance and helpful discussions and Dr. Sven Sewitz for careful reading of the manuscript. We thank CRUK for support (project grant to S.B. and program grants to both S.N. and S.B.).

REFERENCES

1. Gellert M, Lipsett MN, Davies DR. Helix formation by guanylic acid. Proc. Natl. Acad. Sci. U.S.A. 1962; 48:2013–2018. [PubMed: 13947099]
2. Hoogsteen K. The structure of crystals containing a hydrogen-bonded complex of 1-methylthymine and 9-methyladenine. Acta Crystallogr. 1959; 12:822–823.
3. Henderson E, Hardin CC, Walk SK, Tinoco I Jr. Blackburn EH. Telomeric DNA oligonucleotides form novel intramolecular structures containing guanine–guanine base pairs. Cell. 1987; 51:899–908. [PubMed: 3690664]
4. Wang Y, Patel DJ. Solution structure of the *Oxytricha* telomeric repeat d[G4(T4G4)3] G-tetraplex. J. Mol. Biol. 1995; 251:76–94. [PubMed: 7643391]
5. Wang Y, Patel DJ. Solution structure of the *Tetrahymena* telomeric repeat d(T2G4)4 G-tetraplex. Structure. 1994; 2:1141–1156. [PubMed: 7704525]
6. Sen D, Gilbert W. Formation of parallel four-stranded complexes by guanine-rich motifs in DNA and its implications for meiosis. Nature. 1988; 334:364–366. [PubMed: 3393228]
7. Marquet R, Baudin F, Gabus C, Darlix JL, Mougel M, Ehresmann C, Ehresmann B. Dimerization of human immunodeficiency virus (type 1) RNA: Stimulation by cations and possible mechanism. Nucleic Acids Res. 1991; 19:2349–2357. [PubMed: 1645868]
8. Macaya RF, Schultze P, Smith FW, Roe JA, Feigon J. Thrombin-binding DNA aptamer forms a unimolecular quadruplex structure in solution. Proc. Natl. Acad. Sci. U.S.A. 1993; 90:3745–3749. [PubMed: 8475124]
9. Cogoi S, Quadrifoglio F, Xodo LE. G-rich oligonucleotide inhibits the binding of a nuclear protein to the Ki-ras promoter and strongly reduces cell growth in human carcinoma pancreatic cells. Biochemistry. 2004; 43:2512–2523. [PubMed: 14992588]
10. Simonsson T, Pecinka P, Kubista M. DNA tetraplex formation in the control region of c-myc. Nucleic Acids Res. 1998; 26:1167–1172. [PubMed: 9469822]
11. Siddiqui-Jain A, Grand CL, Bearss DJ, Hurley LH. Direct evidence for a G-quadruplex in a promoter region and its targeting with a small molecule to repress c-MYC transcription. Proc. Natl. Acad. Sci. U.S.A. 2002; 99:11593–11598. [PubMed: 12195017]
12. Sun D, Guo K, Rusche JJ, Hurley LH. Facilitation of a structural transition in the polypurine/polypyrimidine tract within the proximal promoter region of the human VEGF gene by the presence of potassium and G-quadruplex-interactive agents. Nucleic Acids Res. 2005; 33:6070–6080. [PubMed: 16239639]
13. De Armond R, Wood S, Sun D, Hurley LH, Ebbinghaus SW. Evidence for the presence of a guanine quadruplex forming region within a polypurine tract of the hypoxia inducible factor 1R promoter. Biochemistry. 2005; 44:16341–16350. [PubMed: 16331995]

14. Giraldo R, Suzuki M, Chapman L, Rhodes D. Promotion of parallel DNA quadruplexes by a yeast telomere binding protein: A circular dichroism study. Proc. Natl. Acad. Sci. U.S.A. 1994; 91:7658–7662. [PubMed: 8052638]
15. Giraldo R, Rhodes D. The yeast telomere-binding protein RAP1 binds to and promotes the formation of DNA quadruplexes in telomeric DNA. EMBO J. 1994; 13:2411–2420. [PubMed: 8194531]
16. Laporte L, Thomas GJ Jr. Structural basis of DNA recognition and mechanism of quadruplex formation by the β subunit of the *Oxytricha* telomere binding protein. Biochemistry. 1998; 37:1327–1335. [PubMed: 9477960]
17. Paeschke K, Simonsson T, Postberg J, Rhodes D, Lipps HJ. Telomere end-binding proteins control the formation of G-quadruplex DNA structures in vivo. Nat. Struct. Mol. Biol. 2005; 12:847–854. [PubMed: 16142245]
18. Kang SG, Henderson E. Identification of non-telomeric G4-DNA binding proteins in human, *E. coli*, yeast, and *Arabidopsis*. Mol. Cells. 2002; 14:404–410. [PubMed: 12521304]
19. Duquette ML, Handa P, Vincent JA, Taylor AF, Maizels N. Intracellular transcription of G-rich DNAs induces formation of G-loops, novel structures containing G4 DNA. Genes Dev. 2004; 18:1618–1629. [PubMed: 15231739]
20. Balagurumoorthy P, Brahmachari SK, Mohanty D, Bansal M, Sasisekharan V. Hairpin and parallel quartet structures for telomeric sequences. Nucleic Acids Res. 1992; 20:4061–4067. [PubMed: 1508691]
21. Mergny JL, Phan AT, Lacroix L. Following G-quartet formation by UV-spectroscopy. FEBS Lett. 1998; 435:74–78. [PubMed: 9755862]
22. Sacca B, Lacroix L, Mergny JL. The effect of chemical modifications on the thermal stability of different G-quadruplex-forming oligonucleotides. Nucleic Acids Res. 2005; 33:1182–1192. [PubMed: 15731338]
23. Mergny JL, Li J, Lacroix L, Amrane S, Chaires JB. Thermal difference spectra: A specific signature for nucleic acid structures. Nucleic Acids Res. 2005; 33:e138. [PubMed: 16157860]
24. Collins I, Weber A, Levens D. Transcriptional consequences of topoisomerase inhibition. Mol. Cell. Biol. 2001; 21:8437–8451. [PubMed: 11713279]
25. Seenisamy J, Rezler EM, Powell TJ, Tye D, Gokhale V, Joshi CS, Siddiqui-Jain A, Hurley LH. The dynamic character of the G-quadruplex element in the c-MYC promoter and modification by TMPyP4. J. Am. Chem. Soc. 2004; 126:8702–8709. [PubMed: 15250722]
26. Chu TY, Besmer P. Characterization of the promoter of the proto-oncogene c-kit. Proc. Natl. Sci. Counc., Repub. China, Part B: Life Sci. 1995; 19:8–18. [PubMed: 7539532]
27. Shaw TJ, Keszthelyi EJ, Tonary AM, Cada M, Vanderhyden BC. Cyclic AMP in ovarian cancer cells both inhibits proliferation and increases c-KIT expression. Exp. Cell Res. 2002; 273:95–106. [PubMed: 11795950]
28. Sakurai S, Fukasawa T, Chong JM, Tanaka A, Fukayama M. C-kit gene abnormalities in gastrointestinal stromal tumors (tumors of interstitial cells of Cajal). Jpn. J. Cancer Res. 1999; 90:1321–1328. [PubMed: 10665649]
29. Yamamoto K, Tojo A, Aoki N, Shibuya M. Characterization of the promoter region of the human c-kit proto-oncogene. Jpn. J. Cancer Res. 1993; 84:1136–1144. [PubMed: 7506248]
30. Yasuda H, Galli SJ, Geissler EN. Cloning and functional analysis of the mouse c-kit promoter. Biochem. Biophys. Res. Commun. 1993; 191:893–901. [PubMed: 7682073]
31. Park GH, Plummer HK III, Krystal GW. Selective Sp1 binding is critical for maximal activity of the human c-kit promoter. Blood. 1998; 92:4138–4149. [PubMed: 9834219]
32. Vandenbark GR, Chen Y, Friday E, Pavlik K, Anthony B, deCastro C, Kaufman RE. Complex regulation of human c-kit transcription by promoter repressors, activators, and specific myb elements. Cell Growth Differ. 1996; 7:1383–1392. [PubMed: 8891342]
33. Huppert JL, Balasubramanian S. Prevalence of quadruplexes in the human genome. Nucleic Acids Res. 2005; 33:2908–2916. [PubMed: 15914667]
34. Todd AK, Johnston M, Neidle S. Highly prevalent putative quadruplex sequence motifs in human DNA. Nucleic Acids Res. 2005; 33:2901–2907. [PubMed: 15914666]

35. Rankin SRAP, Huppert J, Zloh M, Parkinson GN, Todd AK, Ladame S, Balasubramanian S, Neidle S. Putative DNA quadruplex within the human c-kit oncogene. J Am Chem Soc. 2005; 127:10584–10589. [PubMed: 16045346]
36. Sawyers CL. Opportunities and challenges in the development of kinase inhibitor therapy for cancer. Genes Dev. 2003; 17:2998–3010. [PubMed: 14701871]
37. Feigon J, Koshlap KM, Smith FW. ^{1}H NMR spectroscopy of DNA triplexes and quadruplexes. Methods Enzymol. 1995; 261:225–255. [PubMed: 8569497]
38. Phan AT, Modi YS, Patel DJ. Propeller-type parallel-stranded G-quadruplexes in the human c-myc promoter. J. Am. Chem. Soc. 2004; 126:8710–8716. [PubMed: 15250723]
39. Ambrus A, Chen D, Dai J, Jones RA, Yang D. Solution structure of the biologically relevant G-quadruplex element in the human c-MYC promoter. Implications for G-quadruplex stabilization. Biochemistry. 2005; 44:2048–2058. [PubMed: 15697230]
40. Phan AT, Mergny JL. Human telomeric DNA: G-quadruplex, i-motif and Watson–Crick double helix. Nucleic Acids Res. 2002; 30:4618–4625. [PubMed: 12409451]
41. Hazel P, Huppert J, Balasubramanian S, Neidle S. Loop-length-dependent folding of G-quadruplexes. J. Am. Chem. Soc. 2004; 126:16405–16415. [PubMed: 15600342]

Europe PMC Funders Author Manuscripts

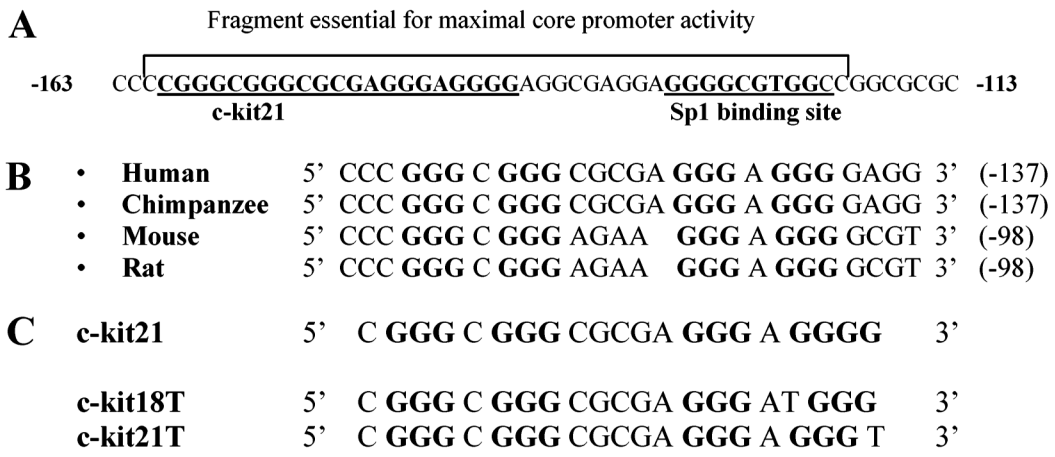

Figure 1.

(A) Positions of the putative quadruplex sequence (c-kit21) and the Sp1-binding DNA sequences within the G-rich strand of the kit promoter. The numbering is relative to the transcription start site (+1). (B) Conservation of the DNA sequence in human, chimpanzee, mouse, and rat. (C) DNA sequences of the native putative quadruplex oligonucleotide c-kit21 and the mutated oligonucleotides c-kit18T and c-kit21T.

Europe PMC Funders Author Manuscripts

Europe PMC Funders Author Manuscripts

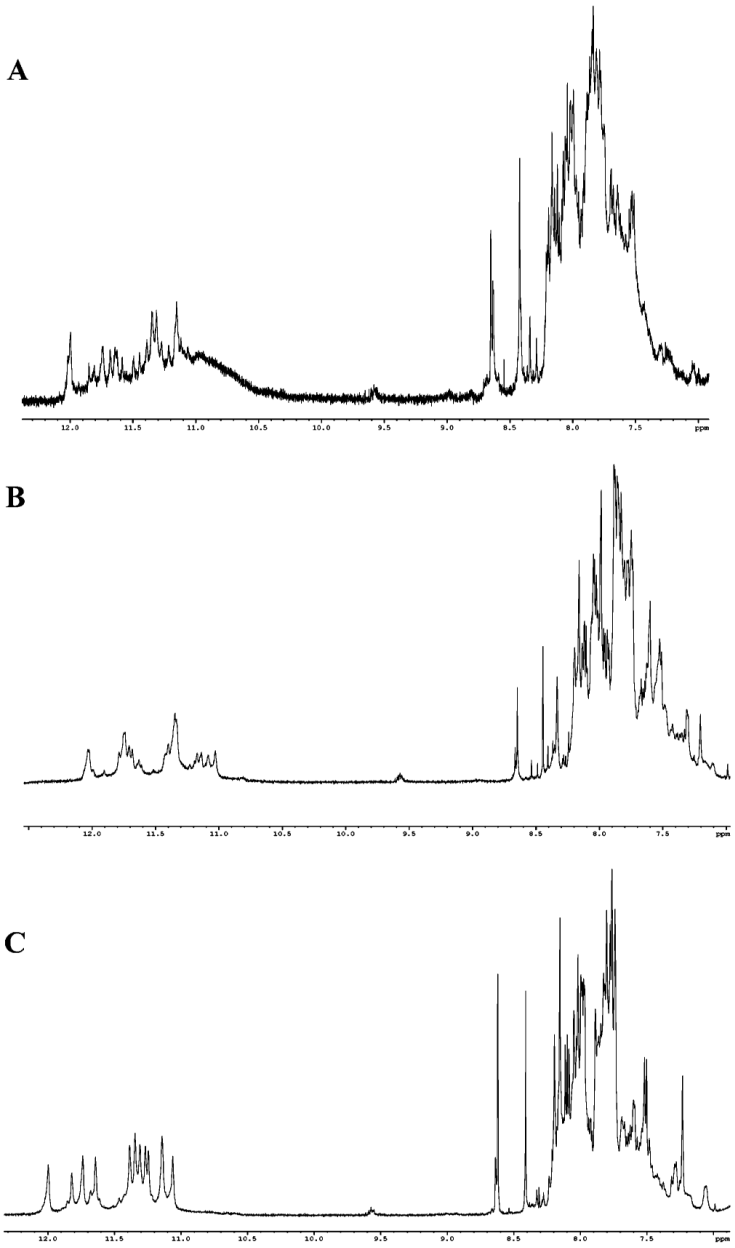

Figure 2.
^{1}H NMR spectra of (A) c-kit21, (B) c-kit18T, and (C) c-kit21T sequences taken in 20 mM potassium phosphate buffer (pH 7.0) at 43 °C.

Europe PMC Funders Author Manuscripts

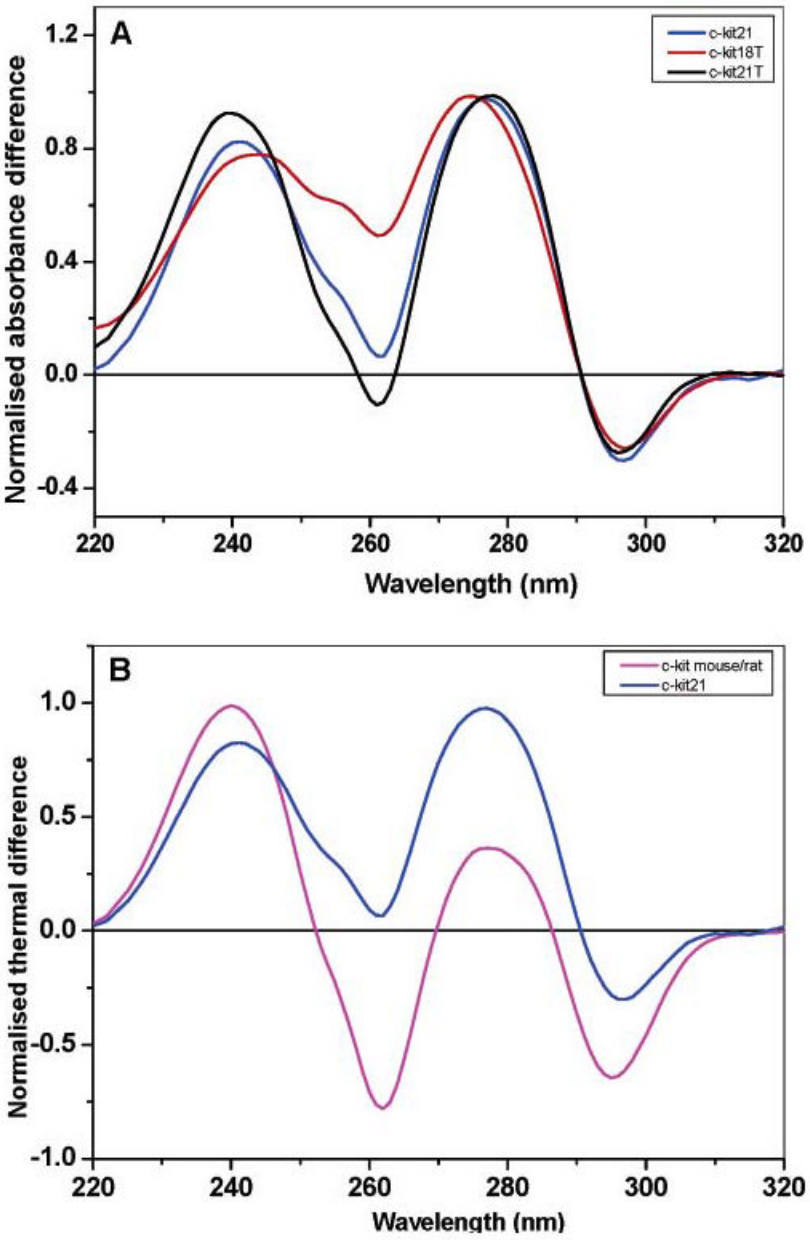

Figure 3.

Normalized UV thermal difference spectra of (A) c-kit18T, c-kit21T, and c-kit21 sequences and (B) mouse/rat c-kit compared with human c-kit21. All spectra were taken in 10 mM Tris-HCl (pH 7.0) containing 100 mM KCl.

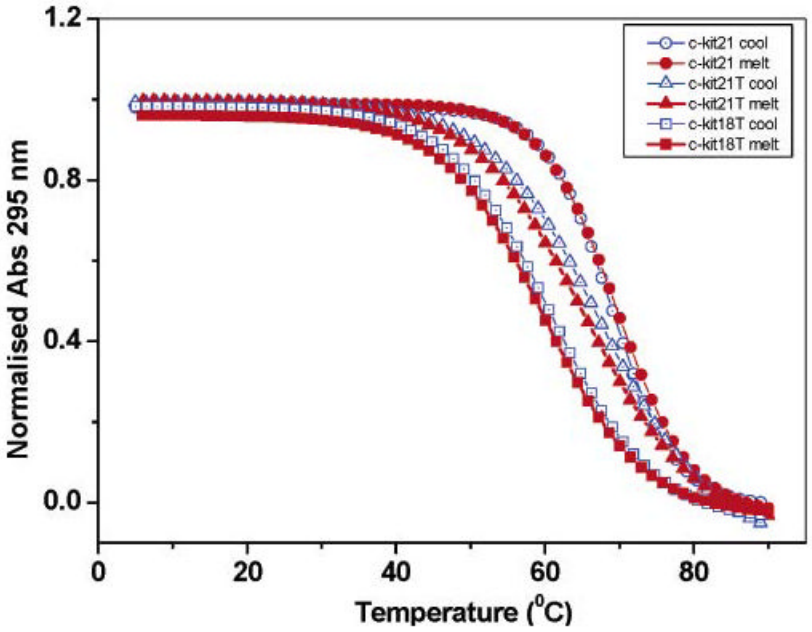

Figure 4.
Normalized UV thermal melting curves of the c-kit21, c-kit21T, and c-kit18T sequences taken in 10 mM Tris-HCl (pH 7.0) containing 100 mM KCl.

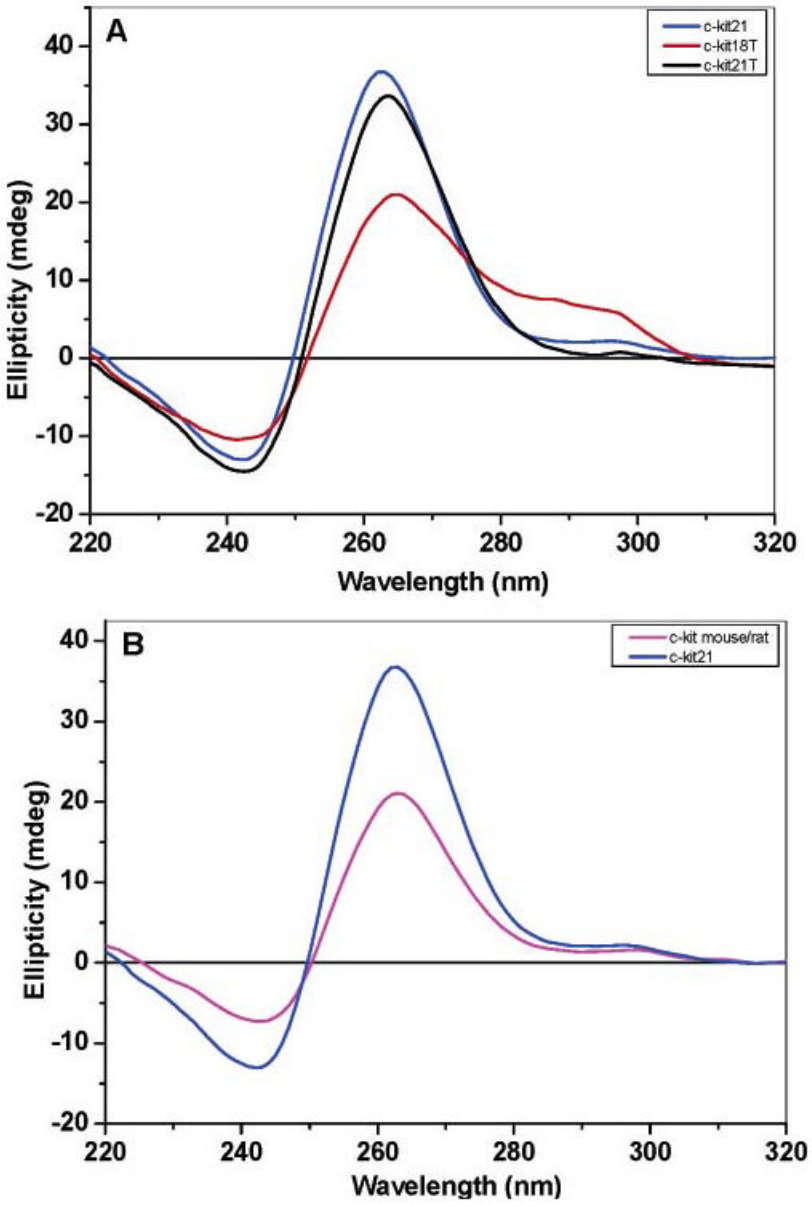

Figure 5.

(A) CD spectra of the c-kit18T, c-kit21T, and c-kit21 sequences. (B) Mouse/rat c-kit compared with human c-kit21. All spectra were taken in 10 mM Tris-HCl (pH 7.0) containing 100 mM KCl at 20 °C.

Europe PMC Funders Author Manuscripts

Table 1

Half-Transition Temperatures ($T_{1/2}$) for c-kit21 with Different Cations at 100 mM Concentrations

cation	$T_{1/2}$ (°C)	cation	$T_{1/2}$ (°C)	cation	$T_{1/2}$ (°C)
K^+	70 ± 1	Na^+	50 ± 1	Li^+	45 ± 1